Role for Dithiolopyrrolones in Disrupting Bacterial Metal Homeostasis

Supporting Information Appendix

Andrew N. Chan, Anthony L. Shiver, Walter J. Wever, Sayyeda Zeenat A. Razvi, Matthew F. Traxler, and Bo Li

Methods

Strains, Media, Culture Conditions and Chemicals

The chemical genomics screen was performed on lysogeny Lenox agar. All other *E. coli* growth assays were performed using lysogeny Miller broth unless otherwise stated. Teknova (Hollister, CA) MOPS minimal media (M2101) supplemented with 0.2% glucose was used for *E. coli* experiments that require specific metal concentrations. Based on the manufacturer's website, this media contains 10 μM $FeSO_4$, 30 nM $CoCl_2$, 10 nM $CuSO_4$ and 10 nM $ZnSO_4$. *E. coli* was cultured at 37 ºC unless otherwise stated. For all metal binding experiments, metal salts ($FeSO_4$, $CuSO_4$ and $ZnSO_4$) were obtained from Sigma-Aldrich at >99% purity. PBS buffer consists of 137 mM NaCl (>99% purity), 2.7 mM KCl (>99% purity), 10 mM Na_2HPO_4 (>98% purity), and 1.8 mM KH_2PO_4 (>99% purity) in ultrapure water (Hydro Ultrapure 18 MΩ.cm Water System). Imipenem (>95% purity) was purchased from GoldBio (St. Louis, MO) and nitrocefin was purchased from CaymanChem (≥95% purity). Trace analysis grade nitric acid from Fisher Scientific was used for ICP-MS analysis. All other chemicals were obtained from Sigma-Aldrich or Fisher Scientific. Holomycin was synthesized as described previously, and NMR and LC/MS analysis confirmed that this holomycin is >99% pure (Fig. S17) (1, 2).

Cloning of the *znuABC* operon and *znuB*

E. coli MG1655 genomic DNA was obtained using the DNEasy Blood and Tissue kit from Qiagen. The *znuABC* operon and *znuB* gene were amplified from MG1655 genomic DNA using the primers indicated in Table S5 and Q5 polymerase (NEB). *ZnuB* was cloned under control of the T5 promoter into the low copy pQE-60 vector (Qiagen) using NcoI and HindIII. The rrnB T1 terminator was amplified from the plasmid pQE-60, and TOPO cloned into pCR-Blunt II (ThermoFisher). The *znuABC* operon was cloned into this vector, using HindIII and NheI sites. This *znuABC* operon linked to the rrnB T1 terminator construct was subcloned into pBR322 between the HindIII and NheI sites.

Cloning and purification of NDM-1

The NDM-1 gene was synthesized by Integrated DNA Technologies (Coralville, IA) and cloned into pET30a digested with NcoI and XhoI. Protein expression in 1L LB was induced in BL-21 (DE3) cells between OD_{600} 0.5 and 0.6 with 0.2 mM IPTG and the induced culture was grown at 18 ºC overnight. Cells were harvested by centrifugation at 6000 rcf. His_6-tagged proteins were purified by nickel affinity chromatography and size exclusion chromatography on an Akta FPLC by the following procedures. The wash buffer contains 50 mM HEPES adjusted to pH 7.5 with NaOH, 300 mM NaCl, 10% glycerol, 25 mM imidazole. The elution buffer is wash buffer with 500 mM imidazole, and the storage buffer contains 50 mM HEPES adjusted to pH 7.5 with NaOH, 150 mM NaCl, 10% glycerol. Cell pellets were lysed in 20 mL buffer containing the wash buffer in addition to 1 EDTA free protease inhibitor tablet (Roche), 1 mM PMSF and 25 μg/mL lysozyme. Cells were lysed using a Branson sonicator at 30% amplitude for 1.5 min of total 'on' time, cycling between 0.5 sec on and 1.5 sec off. Cell debris were subsequently pelleted at 35k rcf and cleared by filtering through a 0.45 μm syringe filter and injected onto an Akta FPLC. Proteins were purified with a GE 5 mL His Trap HP Column with a gradient elution to 500 mM imidazole. Fractions containing the proteins of interest were identified by SDS-PAGE and pooled together for application to a GE Superdex 200 size exclusion column for further purification into storage buffer.

Cloning and purification of FbaA

The *E. coli* FbaA gene was cloned from MG1655 gDNA into pET11a digested with NdeI and BamHI using the primers indicated in Table S5. Protein expression in 1L LB was induced in BL-21 (DE3) cells between OD_{600} 0.5 and 0.6 with 0.2 mM IPTG then grown at 18 ºC overnight. Cells were harvested by centrifugation at 6000 rcf. Proteins were purified by anion exchange chromatography and size exclusion chromatography on an Akta FPLC. The wash buffer contains 20 mM Tris adjusted to pH 7.5 with HCl, 5 mM ZnSO4. The elution buffer is wash buffer with 1 M NaCl, and the storage buffer contains 50 mM Tris pH 7.5, 150 mM NaCl, 10% glycerol. Protein purification follows the general procedure as described above for NDM-1, with the exception of substituting the HEPES buffers with Tris buffers. A GE 5 mL HiTrap Q HP Column was used for anion exchange chromatography and the protein was eluted in a gradient from 0.15 M to 1 M NaCl. Fractions containing the proteins of interest as identified by SDS-PAGE were applied to a GE Superdex 200 size exclusion column for further purification into storage buffer.

Chemical Genomics

The chemical genomic screen was performed as described previously (3-6). Briefly, the mutants from the Keio Collection were grown to a 1–2 mm colony size on the surface of LB agar plates containing antibiotics at defined concentrations as previously described (7). Differences between the wild type and hypersensitive or hyperresistant mutant *E. coli* can be discerned at this size range. Images were taken of the colony arrays, subjected to image analysis using Iris to calculate colony opacity (8), and fitness-scores were calculated using an in-house MATLAB analysis pipeline (https://github.com/AnthonyShiverMicrobes/fitness_score) built from the E-MAP toolbox (5) and adapted for the analysis of *E. coli* K-12 using Iris**.** Data were visualized using Cytoscape, Cluster 3.0, and Java Treeview (9-11). To determine clustering of significant groups of antibiotics, we employed Pearson's correlation with a non-parametric cutoff that allowed for a $p<0.05$.

MIC Determination

An overnight culture of *E. coli* MG1655 grown in 0.2% glucose 1x MOPS Minimal Media (Teknova; Hollister, CA) was diluted to an OD_{600} of 1.0 or approximately 10^8-10^9 cfu/mL with fresh media. A series of media were prepared with varying concentrations of holomycin. For each concentration, stock holomycin was diluted with DMSO such that the same volume would be added to each 5 mL culture. Prepared media was inoculated with 25 µL of the OD_{600} 1.0 culture or approximately a final concentration of 10^5 cfu/mL. Cultures were incubated in a roller drum at 37 °C for 24 h before final OD_{600}'s were measured. The lowest concentration of holomycin at which no growth occurred was assigned as the MIC (0.2 µg/mL) (12-14).

Synergy Testing

Klebsiella pneumoniae BAA-2146 was cultured in MOPS minimal media in a similar manner as *E. coli*. 5 x 5 checkerboards were set up in 1 mL culture volumes, by diluting an overnight culture to a 0.5 McFarland standard and further diluting 1:10 in MOPS MM. Each well in the 5 x 5 panel was treated with varying concentrations of holomycin and incubated for 1.5 h at 37 ºC with shaking at 250 rpm. Following the initial incubation with holomycin, 1 mM DTT and serial dilutions of meropenem were added to each well and the cultures were grown for another 20

h. Culture growth was assessed visually and measured by optical density at 600 nm. MICs and Fractional Inhibitory Concentrations (FICs) were determined as described by Isenberg et al. (15).

P1 Transduction and Construction of Clean Gene Deletion Strains

$P1_{vir}$ lysates of Keio Collection mutants were prepared to move the knocked-out alleles from BW25113 to MG1655 (7). An overnight culture of the BW25113 Keio mutant was inoculated into fresh LB with 10 mM $CaCl_2$ and 0.2% glucose, 1:100. Cultures were incubated at 37 ºC for 30 min before 50 µL of $P1_{vir}$ phage was added and incubated for a further 6 h. Phage was harvested via the addition of a few drops of chloroform. Overnight cultures of MG1655 were resuspended in 0.5 volumes of P1 salts (5 mM $MgSO_4$, 10 mM $CaCl_2$). The resuspended cells were aliquoted as 200 µL reactions, to which 150-200 µL of Keio $P1_{vir}$ lysate was added. The phage-inoculated cultures were incubated at room temperature for 10 min. Subsequently, 500 µL of LB was added to the culture, which was incubated at 37 ºC in a roller drum for 20 min. Cells were pelleted by low-speed centrifugation and resuspended in 200 µL of LB containing 10 mM sodium citrate. Transduced cells were plated on kanamycin selection plates with 10 mM sodium citrate (16, 17). The kanamycin resistance gene was excised using standard flippase protocols to generate clean Keio deletion mutants (7, 18).

Confirmation of Chemical Genomics Screen / Spot Serial Dilution Plates

Strains were grown overnight in MOPS MM. The following day, cultures were normalized to an OD_{600} of 1.0, and then serially diluted from 1 to 10^{-6} into MOPS MM. Using a multichannel pipette, a sample of 5 µL of each dilution was spotted onto MOPS MM agar plates containing 0.1, 0.2, 0.3 and 0.4 µg/mL of holomycin. Plates were dried for 30–45 min in a laminar flow hood then grown for 24 h at 37 ºC before imaging and analysis. In the case of the complementation plates, ampicillin (100 µg/mL) was added in the agar to maintain plasmid selection.

Antimicrobial Activity of Pre-formed *red*-holomycin and Zn-[*red*-holomycin]$_2$ Complex

E. coli MG1655 was grown overnight in MOPS MM. The following day, cultures were diluted 1:20 in MOPS MM. A 100 µL aliquot of this dilution was spread onto a MOPS MM agar plate and allowed to dry at 37 ºC for 30 min. Meanwhile, 10 µL solutions were prepared containing (**1**) 2 mM TCEP, 1 mM $ZnSO_4$, (**2**) 2 mM TCEP, 500 µM holomycin, (**3**) 500 µM holomycin, (**4**) 500 µM holomycin, 2 mM TCEP, 1 mM $ZnSO_4$, (**5**) 500 µM holomycin, 1 mM $ZnSO_4$. Each solution was buffered by 50 mM HEPES pH 7.2. To each plate 5 paper discs were added, each applied with 10 µL of samples 1 through 5. Plates were incubated overnight at 37 ºC and imaged the next day (Fig. S2).

Cellular Metal Content – ICP-MS Sample Preparation

E. coli MG1655 was grown overnight in MOPS MM. The following morning 25 mL of MOPS MM was inoculated with the overnight culture by 1:100 dilution and grown at 37 ºC with shaking at 250 rpm until reaching an OD_{600} of 0.3–0.4. At this point holomycin or DMSO vehicle was added to each 25 mL culture, resulting in a concentration of 0.4 µg/mL holomycin in the treated samples. The cultures grew for another hour, which is about 1 doubling time for *E. coli* under this growth condition. Final OD_{600} values were measured and cultures were pelleted at 4000 rcf. Each pellet was washed twice with 1 volume of PBS containing 1 mM EDTA followed by another two washes of

PBS without EDTA to remove metal ions loosely associated with the cell surface. Final cell pellets were dried down in pre-weighed microcentrifuge tubes using a GeneVac for 3 h and the dry pellet weight was calculated by subtracting the tube weight from the final weight. Dried pellets were dissolved overnight (16 h) in 143 µL of TraceMetal Grade Nitric Acid (Fisher Scientific), and subsequently heated at 80 ºC for 1 h before dilution to 5% nitric acid with Thermo NERL High Purity Water. Samples were submitted to the Mass Spectrometry Facility at the University of North Carolina at Chapel Hill Department of Chemistry for metal content analysis on a Thermo Scientific Element XR ICP-MS instrument.

Holomycin Titration Assays

Metal binding assays were performed as described by Bandara et al. (19, 20). For the aerobic experiments, spectra were recorded by a Cary 50 or Cary 300 UV/Vis spectrophotometer with a 1 cm quartz cuvette. Each titration was conducted in a reaction volume of 1 mL of PBS. For the 4-(2-pyridylazo)-resorcinol (PAR) competition assays, 30 µM PAR was added followed by 10 µM $ZnSO_4$ and 100 µM Tris(2-carboxyethyl)phosphine (TCEP) or 1,4-dithiothreitol (DTT). Holomycin in either 100% DMSO or 100% acetonitrile was titrated into this solution and mixed by pipetting. After the addition of each component a spectrum was recorded from 200 to 800 nm. The same procedure was used for the direct titrations with Zn(II), Fe(II) and Cu(I); $ZnSO_4$, $FeSO_4$, $CuSO_4$ was titrated into 50 µM holomycin with 100 µM TCEP (plus 100 µM ascorbate for Fe(II) and Cu(I) titrations). Data from the competition assays were analyzed by SpecFit Global Analysis Fitting Software (21). Incorporation of $Zn(PAR)_2$ and Zn(PAR) apparent affinity constants of $\log\beta'_2 = 12.34$ and $\log K'_1 = 6.6$, respectively, returned a $\log\beta'_2$ value of 14.8 ± 0.1, for the average of three independent titrations (19, 20, 22).

Reactivity of Holomycin and Zn(*red*-holomycin)$_2$ Complex with Physiological Reductants

The ability of physiological reductants to reduce holomycin was assayed in a similar manner to the titration method for metal binding. In 1 mL of PBS containing 50 µM holomycin; cysteine, glutathione (oxidized and reduced forms) or citric acid were titrated to 2 mM final concentration and the absorbance spectrum of the resulting mixture from 200 to 800 nm was measured. To evaluate the stability of the Zn(*red*-holomycin)$_2$ complex in the presence of cysteine, glutathione (oxidized and reduced forms) or citric acid, holomycin was first reduced with TCEP and the complex was generated by adding 0.5 equivalents of $ZnSO_4$, and subsequently, the same titration assay as above was performed.

pH screen and Extinction Coefficient of Zn(*red*-holomycin)$_2$ Complex

The formation of Zn(*red*-holomycin)$_2$ complex was assessed at varying pH's in PBS buffer. Briefly, a solution of 25 µM holomycin was made in 1 mL of PBS and then reduced by 2 molar equivalents of TCEP. The formation of the complex was determined by the addition of 0.5 equivalents of $ZnSO_4$ and the absorbance of the resulting mixture was measured from 200 to 800 nm. The stability of the complex in solution was determined by following the absorbance over time; the complex is stable for at least 1.5 h.

The extinction coefficient for the Zn(*red*-holomycin)$_2$ complex was determined by titrating holomycin into PBS containing 60 μM $ZnSO_4$ and 100 μM TCEP. Graphpad Prism 6.0 was used to calculate the extinction coefficient by fitting to Beer's Law.

Calculation of pZn for Zn(*red*-Holomycin)$_2$

The formation constant (logβ'_2) determined with SpecFit, was used to calculate a pZn value, which is representative of the free zinc in solution upon chelator treatment (20). Briefly, pZn is defined by **(eq. 1)**. If the concentrations of free zinc, total holomycin and total zinc are defined by x, y, and z as in **(eq. 2)**, the overall formation of the Zn(*red*-holomycin)$_2$ complex is governed by the reaction in **(eq. 3)**, which defines the formation constant in **(eq. 4)**. In this solution the total zinc concentration (z) is equal to the sum of that which is free (x) and that which is bound by holomycin **(eq. 5)**. Substitution and rearrangement yield **(eq. 6)** and **(eq. 7)**. The analogous manipulations can also be performed with the holomycin concentration yielding **(eq. 8)** and **(eq. 9)**. Rearrangement of **(eq. 9)** yields **(eq. 10)**, which is substituted into the equilibrium equation **(eq. 4)** with the values of **(eq. 2)** and **(eq. 7)**. Setting **(eq. 4)** equal to β'_2 and solving for x yields 2.36 x 10^{-11} M, which when substituted into **(eq. 1)**, yields a pZn of 10.6.

$\text{Ligand } [\text{Holo}_{\text{Total}}]: 10\ \mu\text{M}$

$\text{Metal } [\text{Zn}_{\text{Totall}}]: 1\ \mu\text{M}$

$\text{pH } 7.4$

$\log \beta'_2 = 14.82 \pm 0.10$

$$\text{pZn} = -\log[\text{Zn}_{\text{free}}] \quad \textbf{(1)}$$

$$\text{Let x} = [\text{Zn}_{\text{free}}] \quad \textbf{(2)}$$

$$\text{Let y} = [\text{Holo}_{\text{Total}}]$$

$$\text{Let z} = [\text{Zn}_{\text{Total}}]$$

$$\text{Zn}_{\text{free}} + 2(\text{Holo}_{\text{free}}) \xrightarrow{K_{ML_2}} \text{Zn(Holo)}_2 \quad \textbf{(3)}$$

$$K_{ML_2} = \frac{[\text{Zn(Holo)}_2]}{[\text{Zn}_{\text{free}}][\text{Holo}_{\text{free}}]^2} \quad \textbf{(4)}$$

$$[\text{Zn}_{\text{total}}] = [\text{Zn}_{\text{free}}] + [\text{Zn(Holo)}_2] \quad \textbf{(5)}$$

$$\text{z} = \text{x} + [\text{Zn(Holo)}_2] \quad \textbf{(6)}$$

$$[\text{Zn(Holo)}_2] = \text{z} - \text{x} \quad \textbf{(7)}$$

$$[\text{Holo}_{\text{total}}] = [\text{Holo}_{\text{free}}] + 2[\text{Zn(Holo)}_2] \quad \textbf{(8)}$$

$$\text{y} = [\text{Holo}_{\text{free}}] + 2(\text{z} - \text{x}) \quad \textbf{(9)}$$

$$[\text{Holo}_{\text{free}}] = \text{y} - 2\text{z} + 2\text{x} \quad \textbf{(10)}$$

$$K_{ML_2} = \frac{z - x}{x(y - 2z + 2x)^2} = 10^{14.82} M^{-2} \quad (11)$$

$$x = 2.36 \times 10^{-11} M$$

$$pZn = 10.6$$

Calculation of pZn for Zn(EDTA)

In order to calculate the pZn for EDTA at pH 7.4, the absolute formation constant (K_f) of Zn(EDTA) needs to be converted into the conditional formation constant (K'_f). Using **(eq. 12)** and the constants in **(eq. 13)** for pH 7.4 we can calculate the fraction of EDTA in the fully deprotonated form **(eq. 14)** (23). Summation of the $\log_{10}$ of $\alpha_{Y^{4-}}$ **(eq. 15)** with the $\log K_f$ of Zn(EDTA) **(eq. 16)** as in **(eq. 17)** yields the conditional formation constant **(eq. 18)**. The pZn for Zn(EDTA) is calculated similar to pZn for Zn(*red*-holomycin)$_2$ with adjustments for the 1:1 equilibrium. Briefly, the overall formation of the Zn(EDTA) complex is governed by the reaction in **(eq. 11)**, which defines the formation constant in **(eq. 12)**. Following the same substitutions as for Zn(*red*-holomycin)$_2$ **(eq. 24-30)**, a free zinc concentration of 3.16 x 10^{-15} M was obtained, which is equivalent to a pZn of 14.5.

Calculation of the EDTA Conditional Formation Constant at pH 7.4

$$\alpha_{Y^{4-}} = \frac{K_1K_2K_3K_4K_5K_6}{[H^+]^6 + [H^+]^5K_1 + [H^+]^4K_1K_2 + [H^+]^3K_1K_2K_3 + [H^+]^2K_1K_2K_3K_4 + [H^+]^1K_1K_2K_3K_4K_5 + K_1K_2K_3K_4K_5K_6} \quad (12)$$

$$pK_1 = 0.0 \quad (13)$$

$$pK_2 = 1.5$$

$$pK_3 = 2.00$$

$$pK_4 = 2.69$$

$$pK_5 = 6.13$$

$$pK_6 = 10.37$$

$$pH = 7.4$$

$$\alpha_{Y^{-4}} = 0.001015874 \quad (14)$$

$$\log \alpha_{Y^{-4}} = -2.993 \quad (15)$$

$$\log K_f = 16.5 \quad (16)$$

$$\log K'_f = \log K_f + \log \alpha_{Y^{-4}} \quad (17)$$

$$\log K'_f = 13.5 \quad (18)$$

Calculation of Zn(EDTA) pZn

$$\text{Ligand } [EDTA_{Total}]: 10\ \mu M \quad (19)$$

$$\text{Metal } [Zn_{Total}]: 1\ \mu M$$

$$\text{pH } 7.4$$

$$\log K'_f = 13.5$$

$$pZn = -\log[Zn_{free}] \quad (20)$$

Let $x = [Zn_{free}]$ **(21)**

Let $y = [EDTA_{Total}]$

Let $z = [Zn_{Total}]$

$Zn_{free} + (EDTA_{free}) \xrightarrow{K_{ML}} Zn(EDTA)$ **(22)**

$$K_{ML} = \frac{[Zn(EDTA)]}{[Zn_{free}][EDTA_{free}]}$$ **(23)**

$$[Zn_{total}] = [Zn_{free}] + [Zn(EDTA)]$$ **(24)**

$$z = x + [Zn(EDTA)]$$ **(25)**

$[Zn(EDTA)]$ z-x **(26)**

$$[EDTA_{total}] = [EDTA_{free}] + [Zn(EDTA)]$$ **(27)**

$$y = [EDTA_{free}] + (z-x)$$ **(28)**

$$[EDTA_{free}] = y-z+x$$ **(29)**

$$K_{ML} = \frac{z-x}{x(y-z+x)} = 10^{13.5} M^{-1}$$ **(30)**

$x = 3.16 \times 10^{-15} M$

$pZn = 14.5$

Mass Spectrometric Confirmation of Complex Formation

Formation of the complex between reduced holomycin and zinc was further validated by mass spectrometry. Holomycin (50 μM) was first reduced by excess TCEP (250 μM) then molar excess (5 eq) $ZnSO_4$ were added to a volume of 0.1% formic acid (FA) in water. A volume of 20 μL of this solution was immediately analyzed using an Agilent Technologies 6520 Accurate Mass QTOF LC/MS with a 50% MeCN, 0.1% FA mobile phase. Negative ion mode ESI mass spectrometry was carried out using the following parameters: flowrate 0.5 mL/min, gas temperature 325 ºC, drying gas 12 L/min, nebulizer 50 psi, fragmentor 175 V, skimmer 65 V, capillary cap 3000 V, octopole RF 750 V.

NDM-1 Activity and Inhibition Assays

NDM-1 kinetics and inhibition assays were conducted in a Grenier UV-Star 96-well plate in a total assay volume of 300 μL. Assays were performed using a Tecan Infinite M1000 PRO plate reader. Before assaying, purified NDM-1 was incubated with 2.5x molar excess of $ZnSO_4$ for 30 minutes on ice. The reconstituted NDM-1 was buffer exchanged into assay buffer to remove excess Zn(II) using a Micro Bio-Spin Column containing Bio-Gel 6 (Bio-Rad; Hercules, CA). Following exchange, the enzyme was diluted to a working stock concentration with assay buffer (50 mM HEPES containing 0.01% Triton X-100, pH 7.2). A typical reaction with imipenem as substrate contained 250 pM NDM-1, 100 μM imipenem, and 50 μM TCEP. Reactions with nitrocefin as substrate contained 1 nM NDM-1, 20 μM nitrocefin and 50 μM TCEP (1 μM $ZnSO_4$ was included in kinetic reactions). TCEP was added to facilitate the reduction of holomycin. Inhibition assays were performed by first pre-incubating the inhibitor on ice with enzyme in the absence of substrate for 10 minutes prior to the addition of substrate and initiation of the assay.
Hydrolysis of imipenem was monitored by its absorbance at 300 nm at 25 ºC while hydrolysis of nitrocefin was monitored at 492 nm at 37 ºC. Kinetic parameters were determined by using 12 different concentrations of

imipenem ranging from 10 nM to 200 μM or nitrocefin ranging from 5 nM to 100 μM. The IC_{50} of holomycin was determined using 11 different concentrations of holomycin (5 nM to 5 μM) while maintaining the substrate concentration at approximately the reported K_M for imipenem (100 μM), and at 20 μM for nitrocefin, used to generate sufficient absorbance signal for detection (24). The kinetics parameters were determined by fitting initial velocity triplicate data to the Michaelis-Menten equation using Graphpad Prism 6.0 (Imipenem: K_M: 127 ± 14 μM, k_{cat}: 378 ± 22 s^{-1}) (Nitrocefin: K_M: 9.3 ± 1.8 μM, k_{cat}: 6.1 ± 0.3 s^{-1}). The IC_{50} value was also determined using Graphpad Prism 6.0, fitting triplicate data to the activity vs. inhibitor concentration plot. An IC_{50} value of 110 nM was obtained for imipenem, and 153 nM for nitrocefin. Despite assaying multiple concentrations of both *red*-holomycin and nitrocefin, we were unable to fit the mode of inhibition for *red*-holomycin into the three classical modes of inhibition (competitive, noncompetitive, or mixed). The significant hill slope (Fig. S12) is congruent with the observed all-or-nothing inhibition observed for nitrocefin. It is possible that the zinc removal mechanism renders a distinct mode of action for *red*-holomycin.

NDM-1 Zinc Content Determined by ICP-MS

NDM-1 was reconstituted with 2.5 molar equivalents of Zn(II) on ice in activity assay buffer lacking Triton X-100 for 1 hour. After buffer exchange to remove unbound zinc as described above, an aliquot of the reconstituted enzyme was treated for 3 hours on ice with 10 molar equivalents of holomycin in the presence of 2 molar equivalents of TCEP relative to holomycin. Holomycin treated NDM-1 were buffer exchanged again to remove any unbound zinc, holomycin or Zn-holomycin complex. The final protein concentrations were determined using a Bradford Assay (Thermo Scientific) with BSA standards. Protein aliquots of 2500 pmol of reconstituted NDM-1 both before and after holomycin treatment were digested in 10% nitric acid at 80 ºC for 1 h. The digested samples were diluted to 5% nitric acid and submitted to the Mass Spectrometry Facility at the University of North Carolina at Chapel Hill Department of Chemistry for analysis on a Thermo Scientific Element XR ICP-MS.

FbaA Activity and Inhibition Assays

To monitor the activity of FbaA purified above, a coupled assay following the oxidation of NADH was utilized. Inhibition assays were set up in a Grenier UV-Star 96-well plate in a total assay volume of 300 μL and measured using a Tecan Infinite M1000 PRO plate reader at 30 ºC. The assay buffer contained 50 mM Tris-HCl at pH 7.5 and 100 mM potassium acetate. A typical reaction included 0.001 U/mL FbaA, 0.3 mM NADH, 0.2 U/mL GDH/TPI (Sigma Aldrich; G1881), and 50 μM TCEP. TCEP was added to the reaction mixture to reduce holomycin. Inhibition assays were performed by first pre-incubating holomycin on ice with FbaA in the absence of substrate for 10 minutes, and 200 μM fructose-1,6-bisphosphate was added to the mixture to initiate the assay. The reaction progress was monitored by the loss of NADH's absorbance at 340 nm. The IC_{50} of holomycin was determined using 11 different concentrations of holomycin (50 nM to 50 μM) while maintaining the substrate concentration at approximately the reported K_M (200 μM) (25). The dose response of FbaA to treatment with holomycin was plotted using GraphPad Prism 6.0.

RNA Polymerase Activity Assays

Purified holo-*E. coli* RNA polymerase was a generous gift from Dr. Dorothy Erie at UNC. The activity assays were conducted as described previously with a few modifications (26-28). Briefly, each 100 µL reaction contained 40 mM Tris pH 8.0, 4 mM $MgCl_2$, 300 mM KCl, 4 mM spermidine, 1 mM DTT, 130 µg/mL calf thymus DNA, 0.7 mM [α-32P] CTP and 8 nM RNA polymerase. A sample of 5 µL of DMSO or inhibitor (holomycin or rifampicin) in DMSO was added to each reaction. Due to the excess DTT in the assay buffer, holomycin becomes reduced once added. Reactions were initiated by the addition of 2.7 mM ATP, 1.4 mM UTP and 1.1 mM GTP. After incubation at 37 ºC for 10 minutes, reactions were quenched by the addition of 200 µL of ice-cold YEP solution (50 mM NaPPi, 50 mM EDTA, 0.5 mg/mL yeast tRNA). Following the quench, nucleic acids were precipitated by addition to 3 mL of ice-cold 5% trichloroacetic acid and incubation on ice for > 10 minutes. The precipitated nucleic acids, which contain the newly synthesized radioactive RNA, were filtered through Whatman GF/C filters and washed with 35 mL of wash buffer (1 M HCl containing 0.1 M NaPPi) followed by 5 mL ethanol. The filters were added to 14 mL of ScintiSafe™ Econo 2 Cocktail and the radioactivity of newly synthesized RNA was counted by a Beckman Coulter LS6500 liquid scintillation counter.

Isolation of Spontaneous Holomycin-Resistant Mutants

Holomycin-resistant *E. coli* MG1655 mutants were isolated on LB agar in the presence of 3 or 4 µg/mL of holomycin. Spontaneous resistant mutants occur at a frequency of 7×10^{-8} at a holomycin concentration of 3 µg/ml. When 4 µg/mL of holomycin was used, only one resistant colony was isolated for every 10^8 to 10^9 of cells. We collected these mutants and confirmed that they are 2-fold more resistant to holomycin in LB media compared to MG1655. Five resistant mutants were submitted for whole-genome sequencing (Ambry Genetics; Aliso Viejo, CA) along with the parent MG1655 strain from our laboratory. Bioinformatic analyses of single nucleotide mutations were carried out using *E. coli* MG1655 as a reference genome (Accession No. NC_000913). These analyses revealed that two of the five mutants contain single nucleotide mutations in gene *gshA*, which encodes for γ-glutamylcysteine ligase, an enzyme in the glutathione biosynthesis pathway. One mutant HR6 contains a mutation that creates an early stop codon at residue 63, completely abolishing the activity of this enzyme. Mutant HR14 has a His to Arg mutation at residue 150, which coordinates Mg^{2+} and is essential for the activity of GshA (29). Both of these mutations are absent in the parental strain. Our *in vitro* data shows that glutathione is unable to directly reduce holomycin at up to 2 mM concentration (Fig. S15) ; however, glutathione may facilitate the intracellular reductive activation of holomycin *in vivo*. As a result, abolishment of glutathione biosynthesis may reduce the amount of intracellular *red*-holomycin present and confer low level of resistance. Another possibility is that glutathione may play a role in zinc homeostasis and the absence of glutathione may alleviate some of the stress from a disrupted metal homeostasis. The primary intracellular reductant for holomycin remains elusive. We were unable to obtain suppressor mutants that are resistant to high concentrations of holomycin.

Figure S1

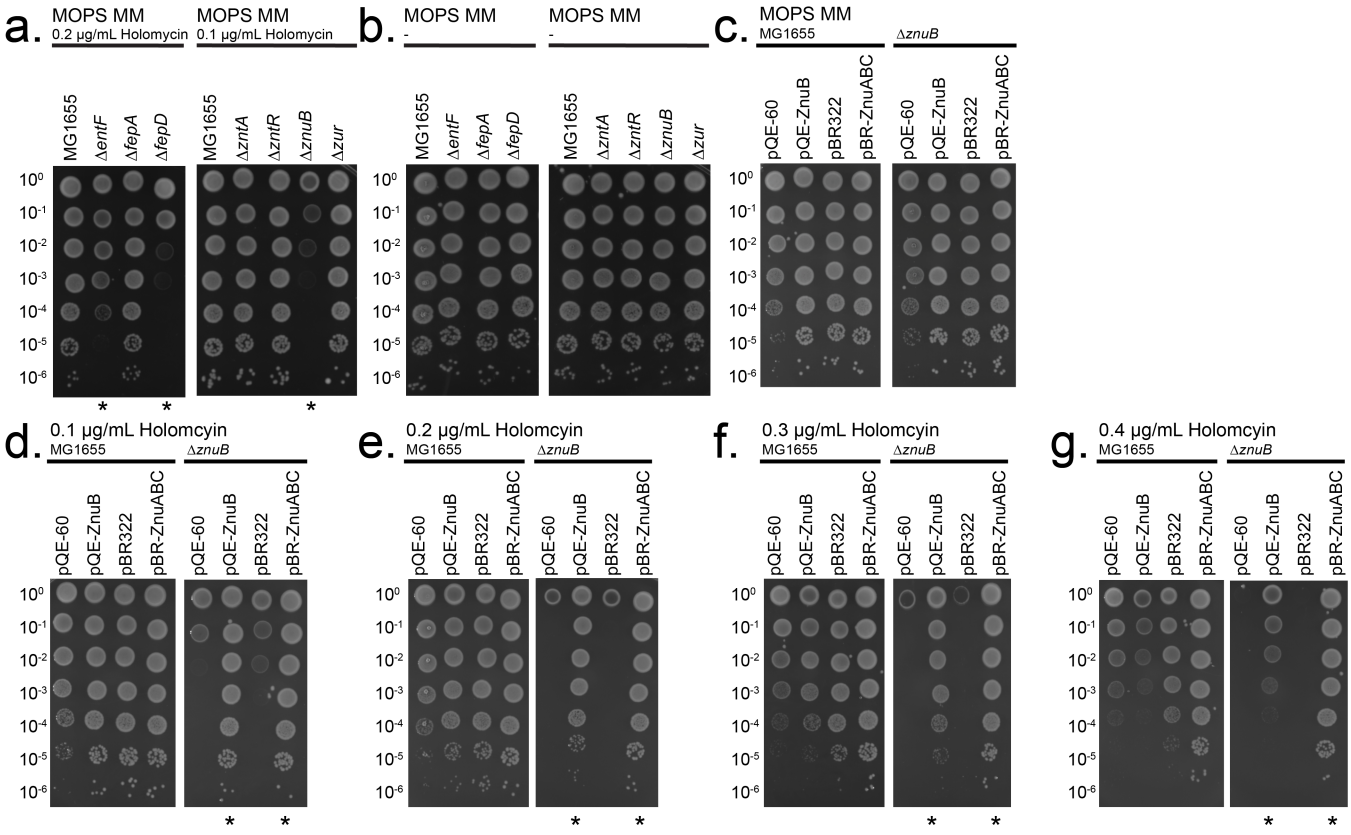

Figure S1. Serial spot dilutions of MG1655 mutants. (a) Iron and zinc homeostasis gene deletions show increased sensitivity to holomycin. Spot serial dilutions for Δ*entF*, Δ*fepA* and Δ*fepD* are plated on 0.2 µg/mL holomycin. Dilutions for Δ*zntA*, Δ*zntR*, Δ*znuB,* and Δ*zur* are plated on 0.1 µg/mL holomycin. The Δ*entF*, Δ*fepD* and Δ*znuB* mutants show increased holomycin sensitivity (*). **(b)** The deletion mutant strains display no inherent growth defects on MOPS agar only. **(c)** Neither complementation with empty vectors (pQE-60, pBR322) nor the complementation vectors (pQE-ZnuB, pBR-ZnuABC) have negative growth effects on MG1655 or Δ*znuB* when plated on MOPS MM. **(d, e, f, g)** In the Δ*znuB* background, complementation with either multiple copies of the whole *znuABC* operon or overexpressed ZnuB rescues the hypersensitive phenotype (*) at 0.1 µg/mL of holomycin (**d**) and enables *E. coli* to survive at a holomycin concentration above the liquid MIC of 0.2 µg/mL (**e, f, g**).

Figure S2

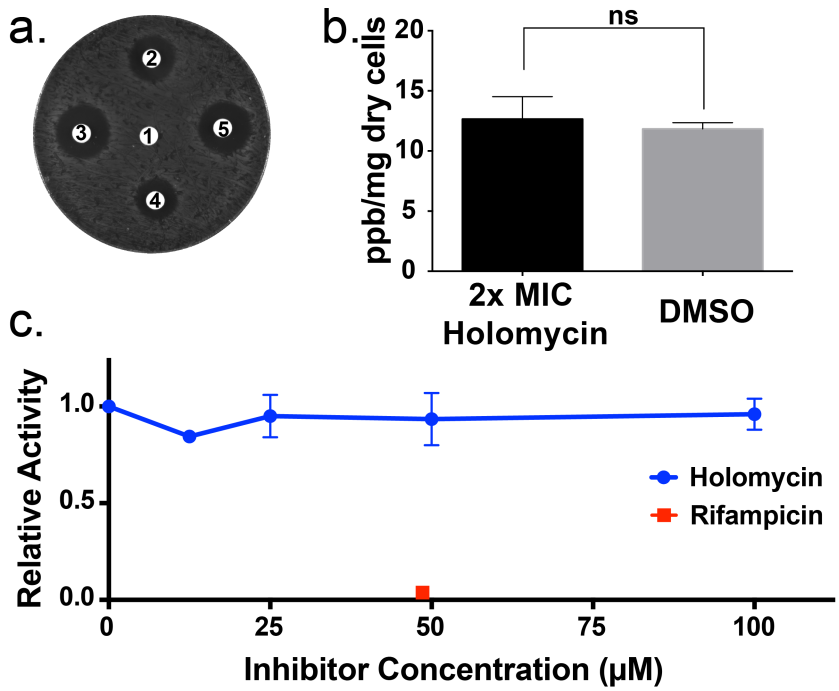

Figure S2. Effect of holomycin on whole cells and RNA polymerase. **(a)** Susceptibility of *E. coli* MG1655 to different forms of holomycin added extracellularly. (**1**) negative control containing 2 mM TCEP and 1 mM $ZnSO_4$, (**2**) reduced dithiol form of holomycin containing 2 mM TCEP and 500 μM holomycin, (**3**) 500 μM disulfide form of holomycin, **(4)** pre-formed Zn(red-holomycin)$_2$ complex containing 500 μM holomycin, 2 mM TCEP, and 1 mM $ZnSO_4$, (**5**) 500 μM holomycin and 1 mM $ZnSO_4$. **(b)** Treatment with holomycin does not change the cellular Zn(II) content of *E. coli* as determined by ICP-MS (ppb Zn/mg dry cells), error bars represent the standard error of the mean of independent samples in triplicates. **(c)** Detection of *E. coli* RNA polymerase activity *in vitro* using a [α-32P] CTP labeled RNA transcription assay. In the presence of excess DTT, holomycin is reduced and does not inhibit RNA polymerase activity from a concentration of 0 μM to 100 μM (21.4 μg/mL), which is 10 times higher than the MIC. A concentration of 49 μM rifampicin was used a positive control, which completely abolishes RNA polymerase activity, error bars represent the standard error of the mean of independent samples in duplicates.

Figure S3

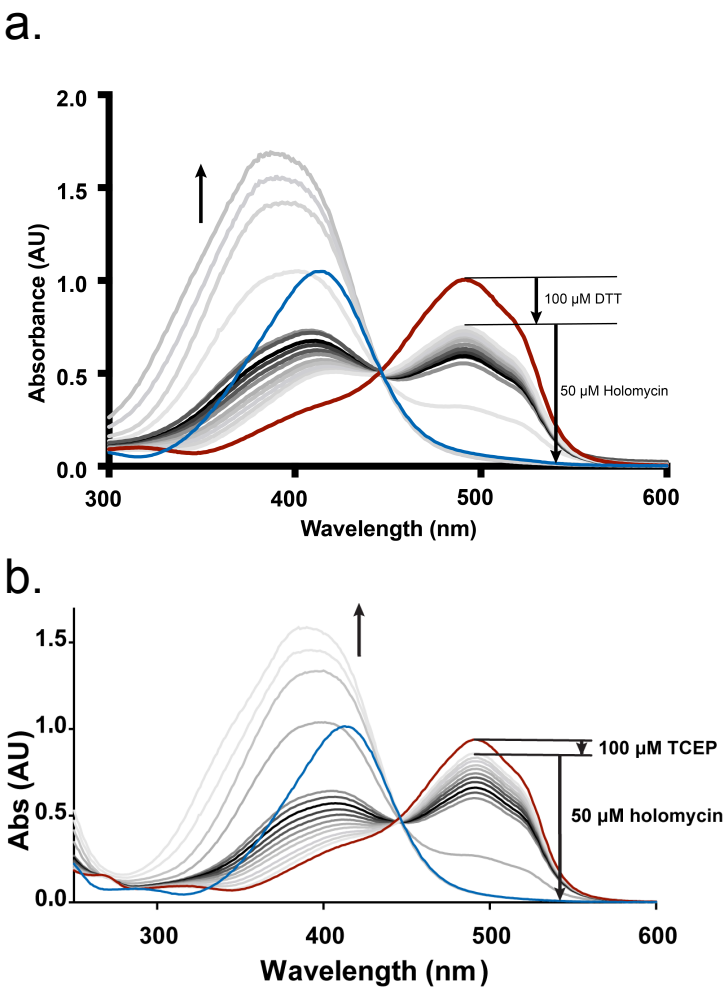

Figure S3. Competitive titration of holomycin into Zn(PAR)$_2$ with DTT (a) and TCEP (b) as the reducing agent. **(a)** PAR alone is shown in blue, 10 µM Zn(PAR)$_2$ is shown in red, 100 µM of DTT was added first, and then holomycin was titrated from 0 to 10 µM in 1 µM steps and from 10 to 50 µM in 10 µM steps shown in grey-black-grey. Notably, addition of DTT alone only partially dissociates the Zn(PAR)$_2$ complex at 493 nm, while addition of holomycin completely dissociates the Zn(PAR)$_2$ complex. The dissociation of the Zn(PAR)$_2$ complex is accompanied by an increase in absorbance between 370 nm to 400 nm as indicated by an arrow, which represents the formation of Zn-(*red*-holomycin)$_2$ complex. (**b**) Similar titration as (**a**) with the exception that DTT is substituted with TCEP, coming from Figure 3a in the main text illustrating that TCEP causes minimal dissociation of Zn(PAR)$_2$.

.

Figure S4

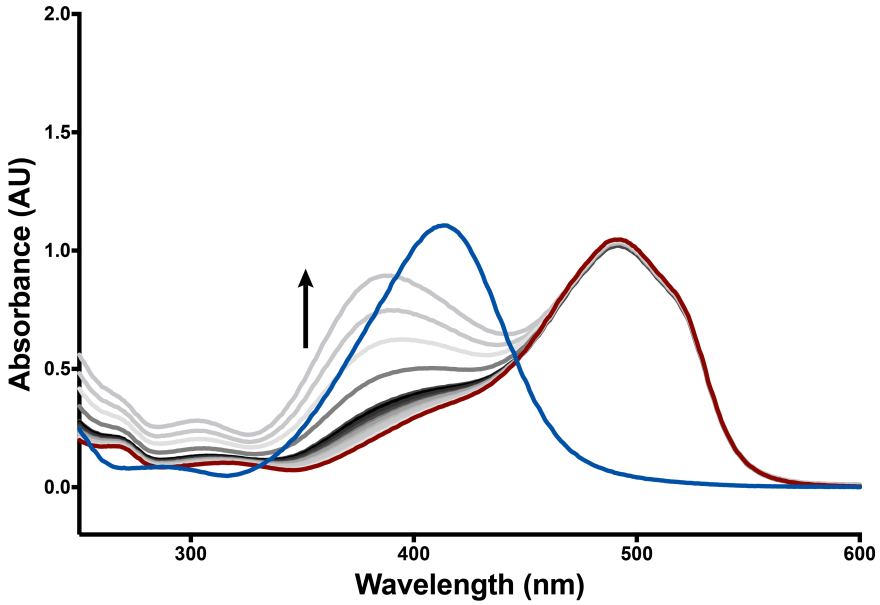

Figure S4. Competitive titration of holomycin into $Zn(PAR)_2$ without reducing agent. PAR alone shown in blue, $Zn(PAR)_2$ shown in red, holomycin is titrated from 0 to 50 μM in grey-black-grey in the absence of reducing agent. No change in absorbance at 493 nm is observed for the $Zn(PAR)_2$ complex, while the peak for holomycin appears at 380 nm, indicating that the disulfide form of holomycin cannot compete with PAR for zinc binding.

Figure S5

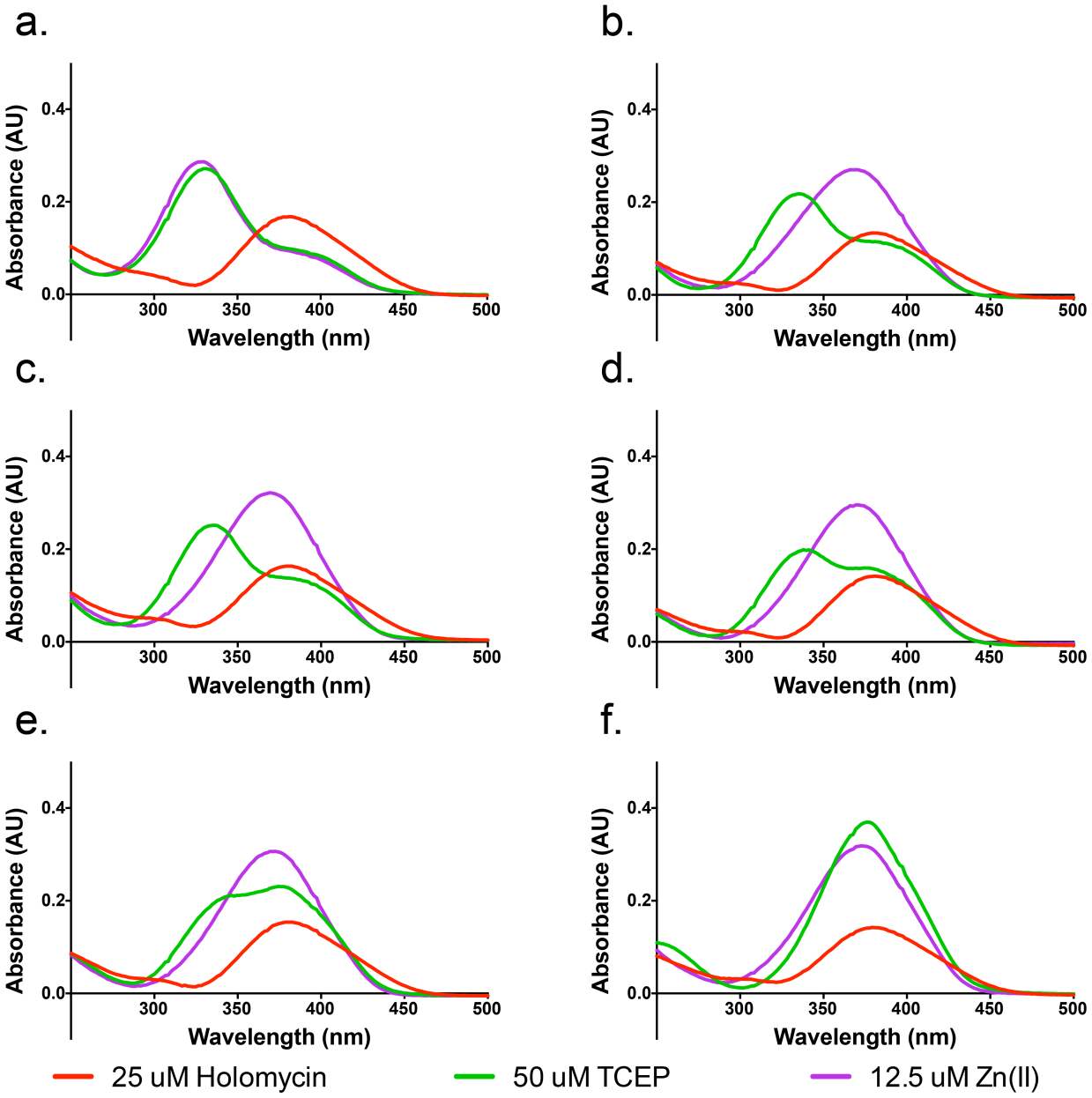

Figure S5. pH Screen for Zn(*red*-holomycin)$_2$ complex formation. In each graph, the trace for 25 μM holomycin in the disulfide form is shown in red. After reduction with 50 μM TCEP (2 equivalents), the trace of red-holomycin is shown in green. Subsequently, the addition of 12.5 μM $ZnSO_4$ (0.5 equivalents) initiates the formation of Zn(*red*-holomycin)$_2$ complex, shown in purple. The pH of the PBS buffers was adjusted to 2 **(a)**, 4 **(b)**, 6 **(c)**, 7.4 **(d)**, 8 **(e)** and 10.5 **(f)**. Formation of the complex is observed from pH 4-10.5 at 375 nm.

Figure S6

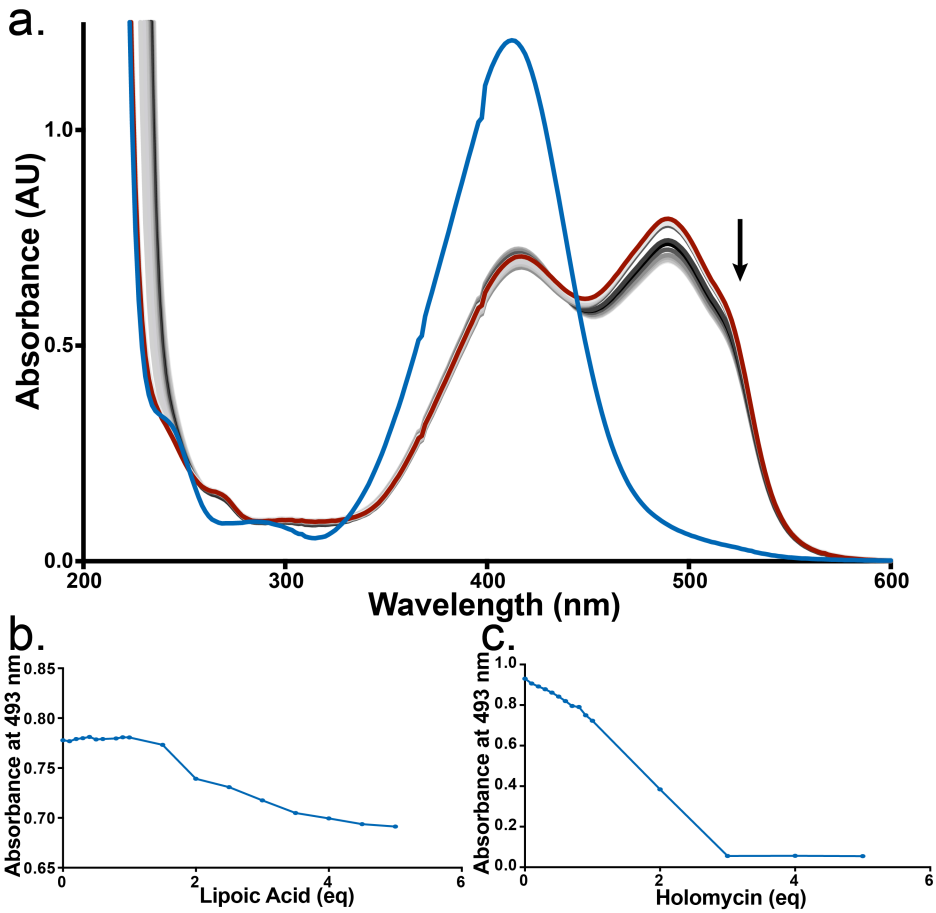

Figure S6. Competitive titration of dihydrolipoic acid into $Zn(PAR)_2$. (**a**) Lipoic acid was reduced by TCEP, and dihydrolipoic acid was titrated into a solution of $Zn(PAR)_2$ and only weakly competes for zinc (down arrow). PAR alone is shown in blue, $Zn(PAR)_2$ in red, and titration of dihydrolipoic acid from 0 to 50 μM is shown in a gray-black gradient. (**b**) The decrease in absorbance at 493 nm of $Zn(PAR)_2$ as dihydrolipoic acid competes for zinc from PAR. (**c**) The decrease in absorbance at 493 nm of $Zn(PAR)_2$ as *red*-holomycin competes for zinc from PAR for comparison. Holomycin is titrated over the same concentration range as dihydrolipoic acid but removes zinc completely from $Zn(PAR)_2$ complex.

Figure S7

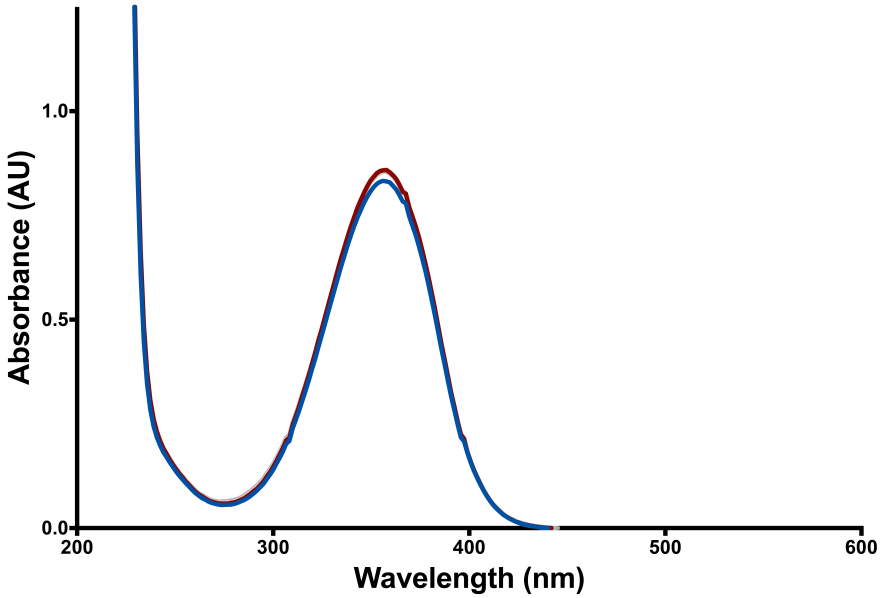

Figure S7. Direct titration of Zn(II) into dimethyldihydroholomycin. The absorbance of dimethyldihydroholomycin at 350 nm is depicted in blue, and the absorbance after Zn(II) addition is depicted in red. No change was observed in the titration, indicating that dimethyldihydroholomycin does not chelate Zn(II).

Figure S8

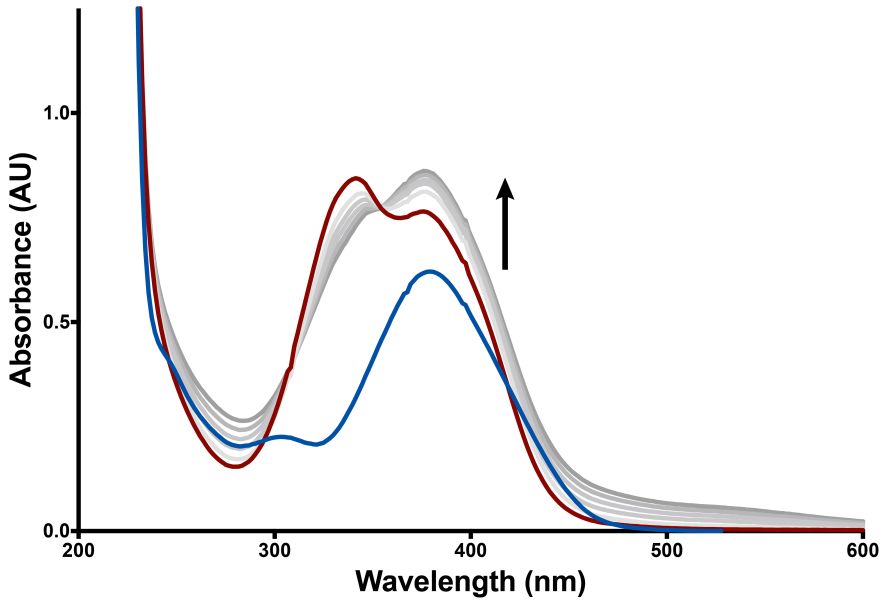

Figure S8. Reduced holomycin binds iron(II) with a λ_{max} at 379 nm. Holomycin (blue) is reduced by TCEP resulting in a change in absorbance pattern for *red*-holomycin (red). Titration traces of Fe(II) are shown in grey, indicating that chelation of Fe(II) by *red*-holomycin results in a λ_{max} shift from 340 nm to 379 nm.

Figure S9

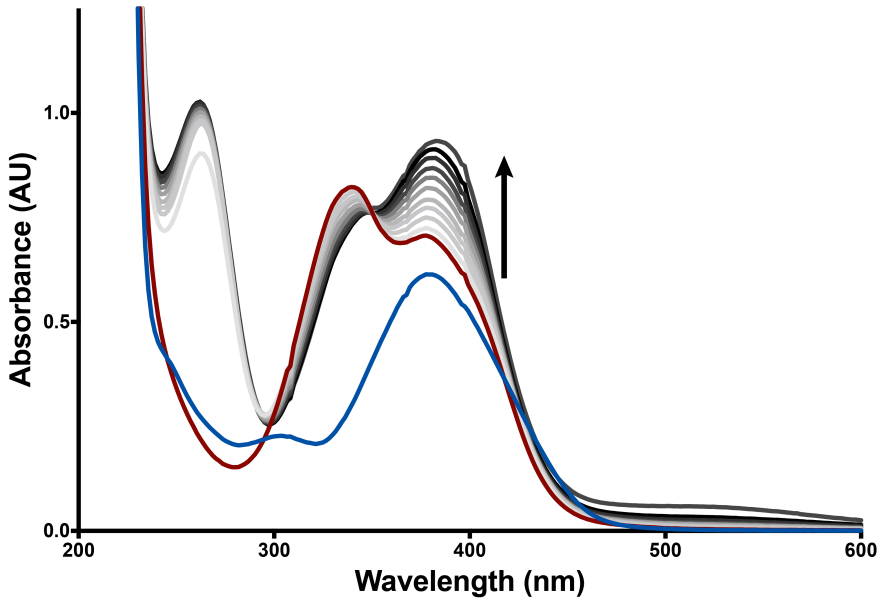

Figure S9. Reduced holomycin binds copper(I) with a λ_{max} at 386 nm. Holomycin (blue) is reduced by TCEP resulting in a change in absorbance pattern for *red*-holomycin (red). Titration traces of Cu(I) are shown in grey to black, indicating that chelation by *red*-holomycin of Cu(I) results in a λ_{max} shift from 340 nm to 386 nm.

Figure S10

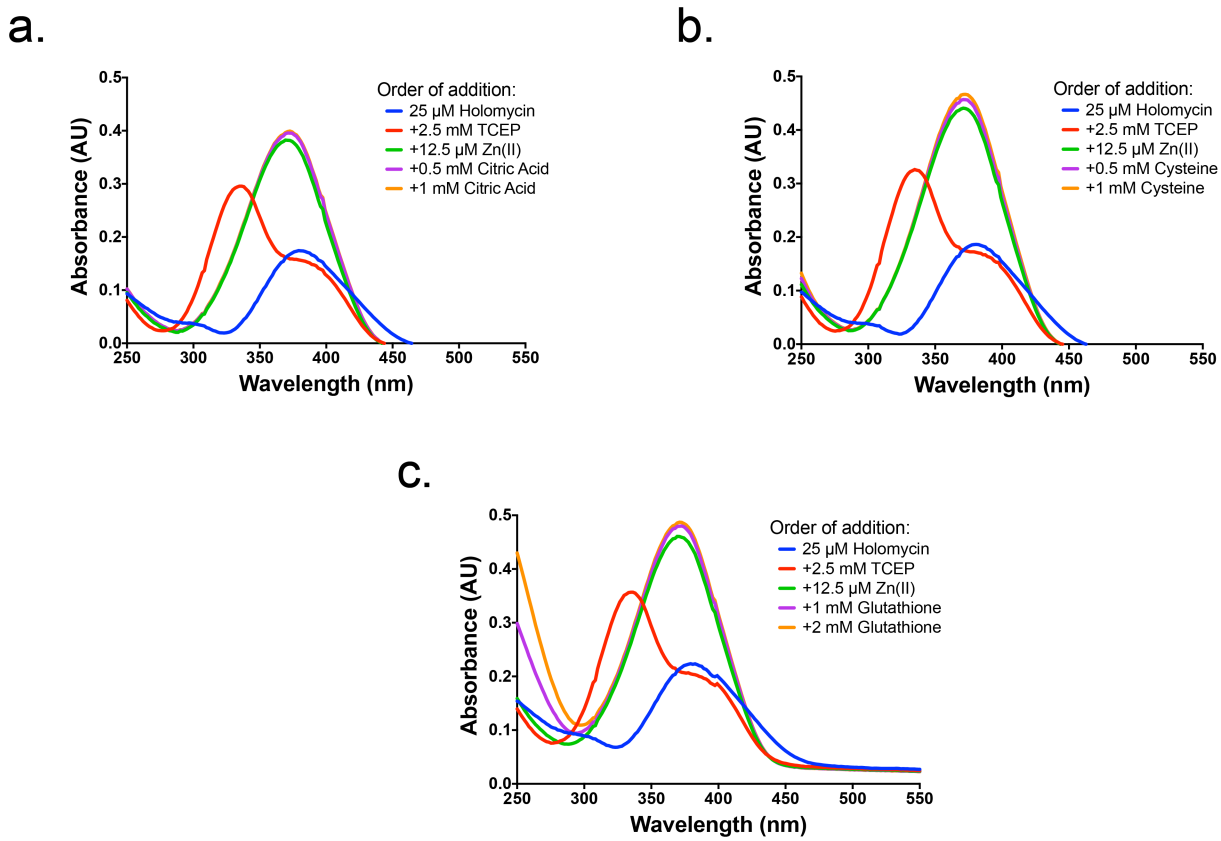

Figure S10. Stability of the Zn(*red*-holomycin)$_2$ complex in the presence of competing physiological ligands at physiologically relevant concentrations. In PBS at pH 7.4, 25 μM holomycin (blue) was reduced by 2.5 mM TCEP to *red*-holomycin (red), which binds 12.5 μM $ZnSO_4$ to generate Zn(*red*-holomycin)$_2$ complex (green). To test the stability of this complex, 0.5 mM citric acid **(a)**, 0.5 mM cysteine **(b)** or 1 mM glutathione **(c)** was added to this solution (traces in purple), followed by addition of more ligands to yield a final concentration of 1 mM citric acid **(a)**, 1 mM cysteine **(b)** and 2 mM glutathione **(c)** (traces in orange). The Zn(*red*-holomycin)$_2$ complex appears stable at 375 nm in the presence of all ligands tested in these graphs.

Figure S11

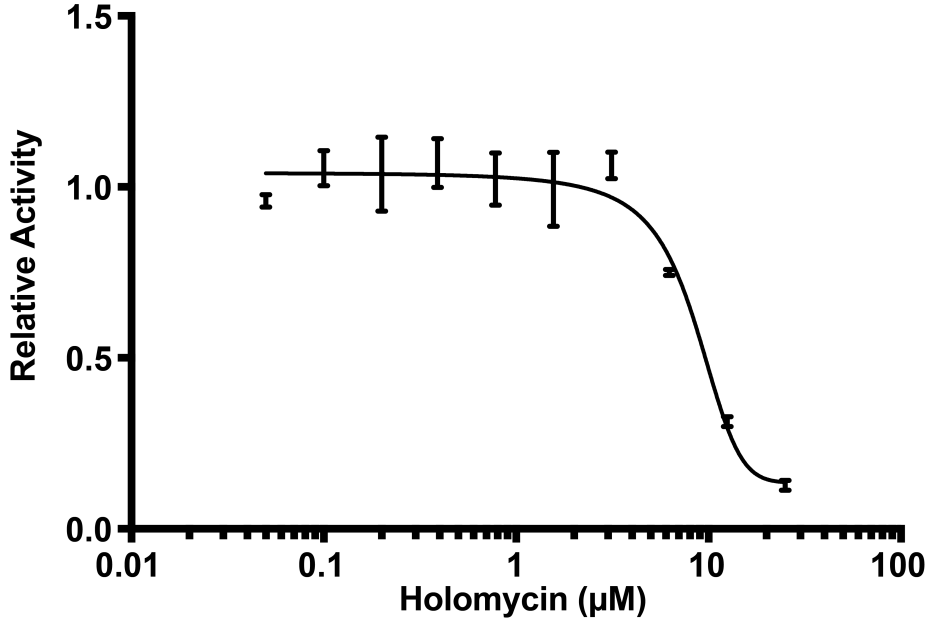

Figure S11. Dose response curve of *E. coli* FbaA inhibition by holomycin. *Red*-holomycin inhibits cleavage of fructose-1,6-bisphosphate by *E. coli* FbaA into dihydroxyacetone phosphate and glyceraldehyde-3-phosphate. The cleavage reaction was coupled with α-glycerophosphate dehydrogenase/triosephosphate isomerase (GDH/TPI) assays. Enzyme activity was monitored by the oxidation of NADH by GDH in the coupled assay. Full activity was defined as the decrease in absorbance at 340 nm of an uninhibited reaction, and the relative FbaA activity at varying concentration of *red*-holomycin is shown in comparison to the full activity. Errors bars represent the standard error of the mean of 3 replicates.

Figure S12

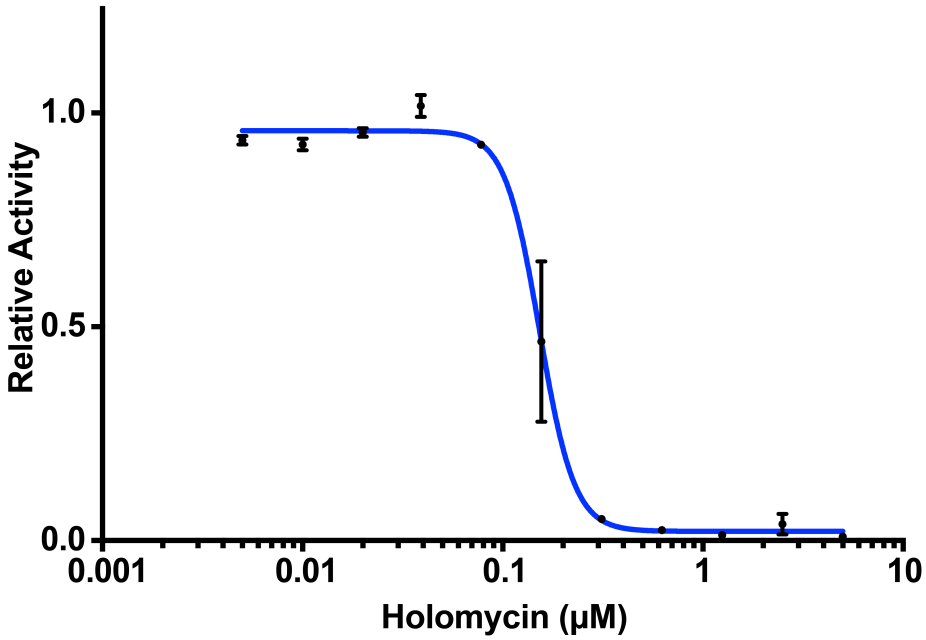

Figure S12. Dose response curve of 1 nM NDM-1 inhibition by varying concentrations of *red*-holomycin using nitrocefin as a substrate. The calculated IC_{50} is 153 nM, the error bars represent the standard error of the mean of 3 replicates, hill slope = -4.996.

Figure S13

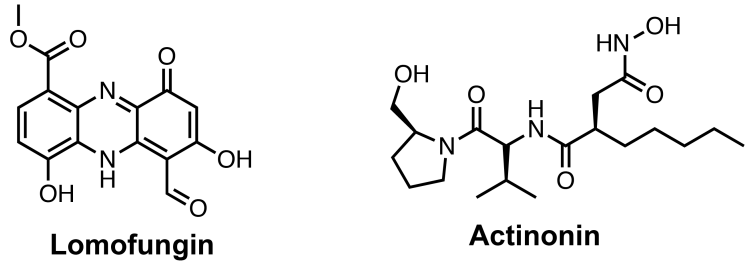

Figure S13. Structures of lomofungin and actinonin, two natural product antibiotics that chelate metal ions. Lomofungin has been proposed to chelate zinc ions from RNA polymerase. Similarly, actinonin chelates metal ions from bacterial peptide deformylase.

Figure S14

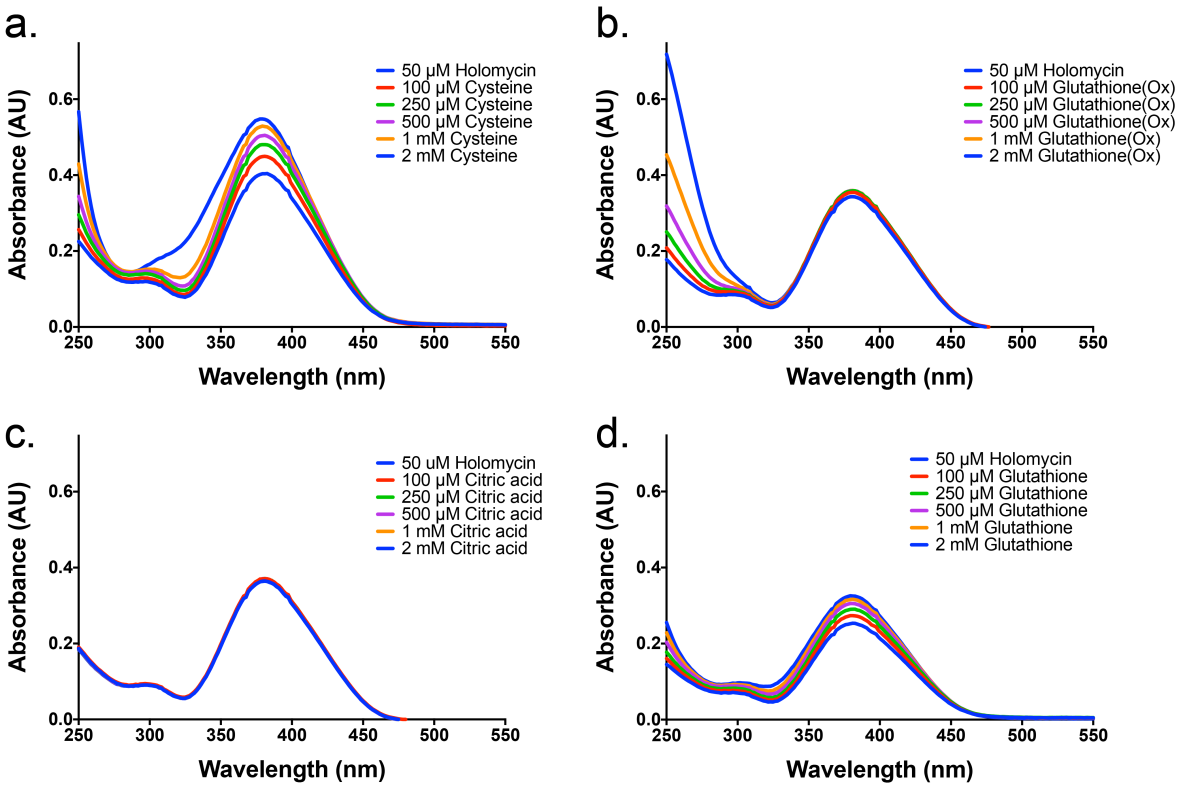

Figure S14. Screen of physically relevant ligands as potential reducing agents for holomycin. Potential cellular reducing agents were titrated in physiologically relevant concentrations from 100 µM to 2 mM into 1 mL of PBS containing 50 µM holomycin at pH 7.4. **(a)** Cysteine titration does not yield any UV shift indicative of *red*-holomycin formation but instead increases the absorbance of the disulfide form of holomycin at the λ_{max}, which may be due to the formation of transient mixed disulfides via disulfide exchange. **(b)** Oxidized glutathione does not reduce holomycin at concentrations up to 2 mM. (**c**) Citric acid does not reduce holomycin at concentrations up to 2 mM. **(d)** Similar to cysteine, the reduced form of glutathione changes the absorbance of holomycin slightly at the λ_{max} but does not convert holomycin to its reduced form.

Figure S15

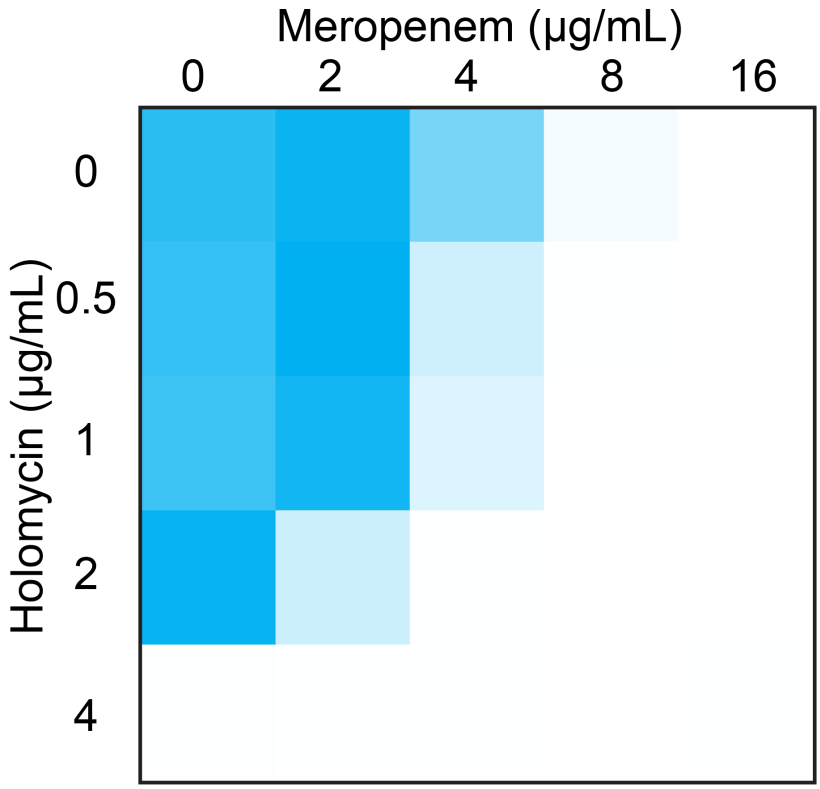

Figure S15. The activities of holomycin and meropenem are additive against *Klebsiella pneumoniae*. Combination treatment of NDM-1 positive *Klebsiella pneumoniae* BAA-2146 with holomycin and meropenem shows an additive effect. Full growth is represented by darker sky blue squares with white denoting the lack of growth. FIC values to quantify the chemical-chemical interaction yielded an FIC index of 1 where < 0.5, 1, and > 2 define synergy, additivity and antagonism, respectively.

Figure S16

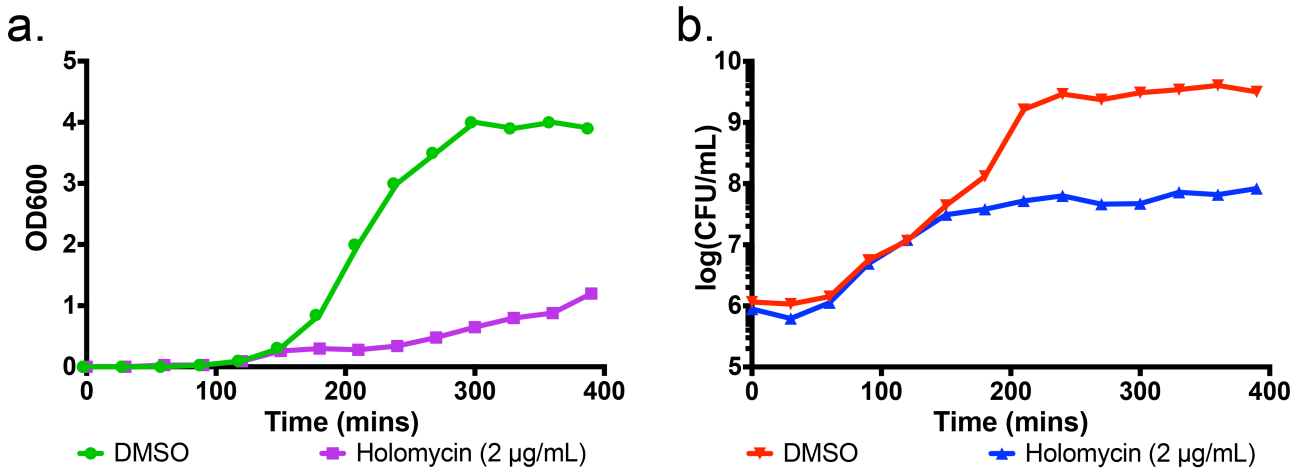

Figure S16. Holomycin is bacteriostatic against *E. coli* MG1655. (a) Growth curve of *E. coli* MG1655 in LB in the presence of holomycin or DMSO control is measured in OD_{600} (2 µg/mL holomycin in purple and DMSO in green) **(b)** Growth curve of *E. coli* MG1655 in LB measured by cfu/mL in the presence of holomycin or DMSO (2 µg/mL holomycin in blue and DMSO in red). Growth curves shown are representatives of several replicate experiments.

Figure S17

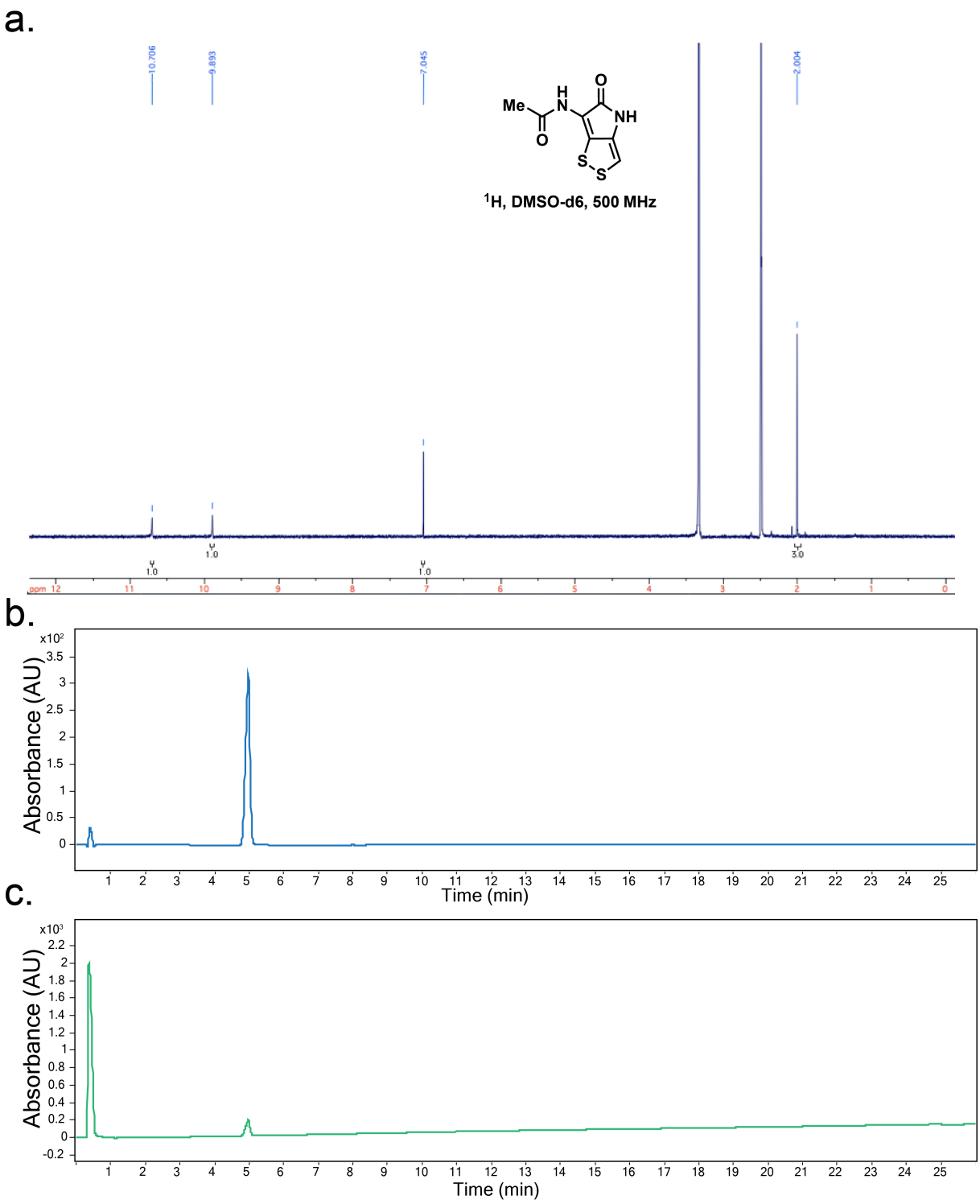

Figure S17. Structure and purity analysis of holomycin used in this study. *N*-(5-oxo-4,5-dihydro-[1,2]dithiolo[4,3-*b*]pyrrol-6-yl)acetamide (Holomycin)**,** prepared according to a literature procedure (2). **(a)** ^{1}H NMR of pure holomycin. ^{1}H NMR (500 MHz; DMSO-d_6) δ 2.00 (s, 3H), 7.04 (s, 1H), 9.89 (s, 1H), 10.71 (s, 1H). UV traces at 390 nm **(b)** and 220 nm **(c)** of synthesized holomycin display a distinct absorbance at 4.9 min retention time. The peak at 0.5 min in (**c**) is also present in "DMSO only" control and comes from the DMSO solvent.

Table S1

Table S1. Conditions for the chemical genomics screen with a total of 57 stress conditions (49 unique conditions).

Condition	Value
D,L-serine hydroxamate	600 µg/mL
M9min casamino acids	0.4 % (w/v)
M9min 7-azatryptophan	14 µg/mL
M9min 5-methylanthranilic acid	20 µg/mL
M9min 5-methyltryptophan	20 µg/mL
M9min glucose-A	0.2% (w/v)
M9min glucose-B	0.2% (w/v)
M9min 5-fluorouridine	250 ng/mL
M9min glucose+UV	0.2% (w/v), 12 sec
M9min 7-azatryptophan	5 µg/mL
M9min glucose	0.2% (w/v)
M9min acetate	0.6% (w/v)
amoxicillin	1.5 µg/mL
ampicillin	4 µg/mL
ampicillin	4 µg/mL
EDTA-A	1 mM
EDTA-B	1 mM
copper(II)	2 mM
acriflavine	10 µg/mL
bile salts	2% (w/v)
SDS+EDTA	0.5% (w/v), 500 µM
SDS-A	1% (w/v)
SDS-B	1% (w/v)
deoxycholate	1% (w/v)
rifampicin	4 µg/mL
clindamycin	64 µg/mL
pseudomonic acid A	36 µg/mL
azelaic acid	1 mg/mL
4C survival	5 wk
pyocyanin	10 µg/mL
gliotoxin-1	10 µg/mL
gliotoxin-2	10 µg/mL
holomycin	2.5 µg/mL
thiolutin	7 µg/mL
silver(II)	1 µM
sodium fluoride	100 mM
bicyclomycin	20 µg/mL
isopropanol	5% (v/v)
t-butanol	5% (v/v)
n-butanol	1% (v/v)
isopentanol	0.5% (v/v)
phenol	0.1% (v/v)
chlorhexidine dihydrochloride	5 µg/mL
A22	5 µg/mL
urea-A	750 mM
urea-B	320 mM
kasugamycin	20 µg/mL

blasticidin S	33 µg/mL
guanidine hydrochloride	30 mM
25C	-
10C	-
UV+10C	12 sec
UV	12 sec
DMSO	9.5% (v/v)
cinoxacin	3 µg/mL
ciprofloxacin	1 ng/mL
tetracycline	500 ng/mL

Table S2

Table S2. Selected genes and fitness scores from the chemical genomics screen.

Genes	Gene Description	Pathway	Holomycin 2.5 µg/mL	Thiolutin 7 µg/mL	EDTA-1 1 mM	EDTA-2 1 mM	Gliotoxin-1 10 µg/mL	Gliotoxin-2 10 µg/mL
entA	2,3-dihydro-2,3-dihydroxybenzoate dehydrogenase	Enterobactin biosynthesis	-0.704	-1.004	-2.658	-4.210	-3.511	-3.115
entB	Isochorismatase, aryl carrier protein	Enterobactin biosynthesis	-2.187	-1.991	-3.637	-4.615	-3.686	-3.352
entC	Isochorismate synthase 1	Enterobactin biosynthesis	-0.932	-1.254	-3.756	-5.193	-3.509	-3.524
entE	2,3-dihydroxybenzoate-AMP ligase	Enterobactin biosynthesis	-1.866	-1.782	-3.676	-3.514	-4.973	-4.334
entF	Serine activating enzyme, peptidyl carrier protein	Enterobactin biosynthesis	-0.964	-2.835	-3.067	-5.738		
fepB	Ferric enterobactin ABC transporter - periplasmic binding protein	FeEnt transport	-0.957	-1.460	-4.508	-8.485	-3.890	-3.557
fepC	Ferric enterobactin ABC transporter - ATP binding subunit	FeEnt transport	-3.050	-2.252	-9.411	-9.753	-3.742	-3.201
fepD	Ferric enterobactin ABC transporter - membrane subunit	FeEnt transport	-0.992	-1.320	-5.328	-8.844	-3.607	-2.986
fepG	Ferric enterobactin ABC transporter - membrane subunit	FeEnt transport	-0.804	-1.893	-5.876	-7.253	-2.124	-1.698
znuA	Zn^{2+} ABC transporter - periplasmic binding protein	Zinc import	-0.878	-2.796	-7.114	-8.502	-5.679	-5.019
znuB	Zn^{2+} ABC transporter – membrane subunit	Zinc import	-1.590	-2.415	-5.554	-6.851	-7.949	-6.739

Table S3

Table S3. Zinc equivalents of ICP-MS analyzed NDM-1 samples after reconstitution and after treatment, errors represent the standard error of the mean.

	Reconstituted (Zn Eq.)	Treated (Zn Eq.)	Change (Zn Eq.)
Sample 1	2.85	0.57	2.28
Sample 2	1.72	0.05	1.67
Sample 3	3.66	1.36	2.30
Sample 4	2.58	0.37	2.21
Mean ± SEM	2.7 ± 0.4	0.6 ± 0.3	2.1 ± 0.5

Table S4

Table S4. Supplementation of media with zinc or iron is unable to significantly rescue growth of *E. coli* MG1655 when treated with holomycin.

Media	OD_{600}	
	0.2 µg/mL Holomycin	DMSO
MOPS only	0.02	0.54
+ 2 µM Zn(II)	0.06	0.51
+ 50 µM Fe(II)	0.01	0.58
+ 2 µM Zn(II) + 50 µM Fe(II)	0.02	0.53

Table S5

Table S5. List of primers used in this study.

Primer Name	Sequence (5' to 3')	Description
AC-0239	GATACAGCTAGCGTTATTGGTGCCCTTAAACG	rrmB T1 Term Fwd NheI
AC-0240	GATACATCTAGAGCGGCGGATTTGTC	rrmB T1 Term Rev XbaI
AC-0241	GATACACACGTGTGCACGTAATCACTTCCTCA	ZnuABC Fwd XhoI
AC-0242	GATACAGCTAGCTGCACGTAATCACTTCCTCA	ZnuABC Fwd NheI
AC-0243	GATACATCTAGACGACAAATGTGTTCAGCGATAG	ZnuABC Rev XbaI
AC-0244	GATACAAAGCTTCGACAAATGTGTTCAGCGATAG	ZnuABC/ZnuB Rev HindIII
AC-0245	GATACACCATGGCTATGATTGAATTATTATTTCCCGG	ZnuB Fwd NcoI
AC-0246	CCCGAAAAGTGCCACCTG	T5 Fwd
AC-0247	GGAGTTCTGAGGTCATTACTGG	T0 Terminator
AC-0248	CTTGTCTGCTCCCGGCATCC	pQE60 Rev
AC-0249	AATAGGCGTATCACGAGGC	pBR322 Fwd
AC-0250	GGTGATGTCGGCGATATAGG	pBR322 Rev
AC-0255a	GATACACATATGTCTAAGATTTTTGATTTCGT	pET11-fbaA Fwd (NdeI)
AC-0256	GATACAGGATCCATCTTACAGAACGTCGATCG	pET-fbaA Rev (BamHI)

Table S6

Table S6. Genes identified by the chemical genomics screen with fitness scores to thiolutin of either >2 or <-2.

Gene	Holomycin 2.5 µg/mL	Thiolutin 7 µg/mL	EDTA-1 1 mM	EDTA-2 1 mM	Gliotoxin-1 10 µg/mL	Gliotoxin-2 10 µg/mL
ybgT		-7.287	-6.023	-4.866	-5.737	-7.193
cydD	-4.175	-6.976	-3.404	-3.746	-8.865	-8.358
cydB	-8.035	-6.579	-2.363	-7.168	-7.402	-7.863
lon	-3.653	-4.913	-1.457	1.551	4.678	0.686
tolC	-0.195	-4.639	1.416	2.029	-5.679	-7.173
nuoB	-2.851	-4.560	-3.349	-1.719	-3.411	-5.022
ubiH	-3.297	-4.544	-0.561	-1.321	-1.808	-2.173
arcB	-1.949	-4.477	-1.970	-1.236	-5.533	-4.278
nuoJ	-2.982	-3.998	-2.817	-1.184	-1.911	-4.891
nuoK	-3.174	-3.646	-2.608	-1.446	-2.003	-4.507
cydA-SPA	-1.093	-3.628	-2.962	-3.835	-2.322	-1.346
ubiX	-1.991	-3.569	-1.128	-0.638	-1.644	-2.370
nfuA	-2.123	-3.502	-0.647	-1.243	-3.166	-2.268
nuoL	-3.109	-3.482	-3.089	-1.349	-2.215	-5.213
fimE	-2.476	-3.453	0.473	-1.881	-0.874	-0.355
ubiF	-2.865	-3.331	-3.481	-2.667	-3.366	-3.601
lrp	-2.329	-3.265	-0.738	-1.557	0.115	-0.973
*yfiO**	-1.104	-3.051	-0.341	0.643	1.090	-0.929
nuoE	-2.488	-3.042	-2.359	-2.335	-1.324	-3.758
pgm	-3.365	-3.036	-2.403	-2.468	1.807	2.209
nuoA	-2.473	-3.015	-2.565	-1.377	-2.110	-4.120
fur	-1.615	-2.975	0.529	-1.643	-1.804	-0.609
nuoC	-1.709	-2.962	-0.517	-0.400	-1.206	-1.850
rplA		-2.871	-2.370	1.418	1.072	0.947
entF	-0.964	-2.835	-3.067	-5.738		
znuA	-0.878	-2.796	-7.114	-8.502	-5.679	-5.019

ycgB		-2.745			-1.647	-2.050
nuoH	-2.430	-2.586	-2.422	-1.036	-1.842	-4.174
rpiB	-0.844	-2.544	0.479	-0.692	-0.031	0.283
ptsI	-1.259	-2.420	0.015	0.422	-1.256	-1.311
znuB	-1.590	-2.415	-5.554	-6.851	-7.949	-6.739
fepC	-3.050	-2.252	-9.411	-9.753	-3.742	-3.201
nuoM	-2.390	-2.219	-2.197	-1.812	-1.621	-3.459
yfiO-DAS	0.324	-2.215		-1.014	-2.121	
ruvC	-1.826	-2.214	-1.279	-0.630	0.535	-0.175
recA	-2.562	-2.211	-0.745	0.511	0.471	-2.117
nuoF	-2.709	-2.199	-2.507	-0.793	-1.516	-3.456
aceE	-1.813	-2.195	-1.314	0.085	-1.692	-2.287
waaF	-2.759	-2.161	1.139	-0.668	-8.441	-11.067
kgtP	-0.914	-2.134	0.262	-0.902	-0.814	-1.329
ygfZ	-2.107	-2.089	-2.168	-1.638	-3.003	-2.561
tdcE	-0.282	-2.087	1.320	-0.269	-0.439	
rpiR	-1.970	-2.083	1.107	0.576	-0.521	-0.248
rssA	-1.032	-2.078	-0.393	0.915	-1.002	-0.549
ygeA	0.223	-2.072	-0.549		-0.274	-0.282
crr	-2.821	-2.044	-1.807	-0.614	-1.853	-1.319
tp2	-1.022	-2.014	-0.876	-1.688	-1.713	-1.325
aceF	-2.008	-2.005	-1.194	0.327	-3.111	-4.434
deaD	-0.548	2.215	-0.798	1.449	2.647	1.774
rfaD	1.267	2.392	1.478	0.914	-1.908	-0.618
yedF	0.256	2.422	-0.424	-0.481	0.820	-0.942
cpsG	2.567	2.494	-3.256	-6.269	2.547	1.570
hfq	2.000	2.576	-1.661	-0.023	-0.088	-0.419

References

1. Li B, Wever WJ, Walsh CT, & Bowers AA (2014) Dithiolopyrrolones: biosynthesis, synthesis, and activity of a unique class of disulfide-containing antibiotics. *Nat. Prod. Rep.* 31(7):905-923.
2. Hjelmgaard T, Givskov M, & Nielsen J (2007) Expedient total synthesis of pyrrothine natural products and analogs. *Org. Biomol. Chem.* 5(2):344-348.
3. Nichols RJ*, et al.* (2011) Phenotypic landscape of a bacterial cell. *Cell* 144(1):143-156.
4. Shiver AL*, et al.* (2016) A chemical-genomic screen of neglected antibiotics reveals illicit transport of kasugamycin and blasticidin S. *PLoS Genet.* 12(6):e1006124.
5. Collins SR, Schuldiner M, Krogan NJ, & Weissman JS (2006) A strategy for extracting and analyzing large-scale quantitative epistatic interaction data. *Genome Biol.* 7(7):R63.
6. Typas A*, et al.* (2008) High-throughput, quantitative analyses of genetic interactions in *E. coli*. *Nat. Methods* 5(9):781-787.
7. Baba T*, et al.* (2006) Construction of *Escherichia coli* K-12 in-frame, single-gene knockout mutants: the Keio collection. *Mol. Syst. Biol.* 2(1):1-11.
8. Paradis-Bleau C, Kritikos G, Orlova K, Typas A, & Bernhardt TG (2014) A genome-wide screen for bacterial envelope biogenesis mutants identifies a novel factor involved in cell wall precursor metabolism. *PLoS Genet.* 10(1):e1004056.
9. Saldanha AJ (2004) Java Treeview--extensible visualization of microarray data. *Bioinformatics (Oxford, England)* 20(17):3246-3248.
10. de Hoon MJ, Imoto S, Nolan J, & Miyano S (2004) Open source clustering software. *Bioinformatics (Oxford, England)* 20(9):1453-1454.
11. Cline MS*, et al.* (2007) Integration of biological networks and gene expression data using Cytoscape. *Nat. Protocols* 2(10):2366-2382.
12. Andrews JM (2001) Determination of minimum inhibitory concentrations. *J. Antimicrob. Chemother.* 48(suppl 1):5-16.
13. Sadaf Q (2007) Macro- and Microdilution Methods of Antimicrobial Susceptibility Testing. *Antimicrobial Susceptibility Testing Protocols*, (CRC Press), pp 75-79.
14. Wiegand I, Hilpert K, & Hancock RE (2008) Agar and broth dilution methods to determine the minimal inhibitory concentration (MIC) of antimicrobial substances. *Nat. Protoc.* 3(2):163-175.
15. Isenberg HD & American Society for Microbiology. (2004) *Clinical microbiology procedures handbook* (ASM Press, Washington, D.C.) 2nd Ed.
16. Moore SD (2011) Assembling new *Escherichia coli* strains by transduction using phage P1. *Methods Mol. Biol.* 765:155-169.
17. Thomason LC, Costantino N, & Court DL (2007) E. coli genome manipulation by P1 transduction. *Current protocols in molecular biology / edited by Frederick M. Ausubel ... [et al.]* Chapter 1:Unit 1.17.
18. Datsenko KA & Wanner BL (2000) One-step inactivation of chromosomal genes in *Escherichia coli* K-12 using PCR products. *Proc. Natl. Acad. Sci. U. S. A.* 97(12):6640-6645.
19. Bandara HM, Kennedy DP, Akin E, Incarvito CD, & Burdette SC (2009) Photoinduced release of Zn2+ with ZinCleav-1: a nitrobenzyl-based caged complex. *Inorg. Chem.* 48(17):8445-8455.
20. Alies B, Wiener JD, & Franz KJ (2015) A prochelator peptide designed to use heterometallic cooperativity to enhance metal ion affinity. *Chem. Sci.* 6(6):3606-3610.
21. Gampp H, Maeder M, Meyer CJ, & Zuberbuhler AD (1985) Calculation of equilibrium constants from multiwavelength spectroscopic data-I mathematical considerations. *Talanta* 32(2):95-101.
22. Hunt JB, Neece SH, & Ginsburg A (1985) The use of 4-(2-pyridylazo)resorcinol in studies of zinc release from *Escherichia coli* aspartate transcarbamoylase. *Anal. Biochem.* 146(1):150-157.
23. Harris DC (2007) *Quantitative chemical analysis* (W.H. Freeman and Co., New York) 7th Ed pp xvi, 663, 619, 621, 631, 633, 610, 621 p.
24. van Berkel SS*, et al.* (2013) Assay platform for clinically relevant metallo-β-lactamases. *J. Med. Chem.* 56(17):6945-6953.
25. Zgiby SM, Thomson GJ, Qamar S, & Berry A (2000) Exploring substrate binding and discrimination in fructose1,6-bisphosphate and tagatose 1,6-bisphosphate aldolases. *Eur. J. Biochem.* 267(6):1858-1868.
26. Chamberlin M, Kingston R, Gilman M, Wiggs J, & deVera A (1983) Isolation of bacterial and bacteriophage RNA polymerases and their use in synthesis of RNA in vitro. *Methods Enzymol.* 101:540-568.
27. Chamberlin MJ, Nierman WC, Wiggs J, & Neff N (1979) A quantitative assay for bacterial RNA polymerases. *J. Biol. Chem.* 254(20):10061-10069.

28. Xue Y, Hogan BP, & Erie DA (2000) Purification and initial characterization of RNA polymerase from Thermus thermophilus strain HB8. *Biochemistry* 39(46):14356-14362.
29. Inoue Y, Iba Y, Yano H, Murata K, & Kimura A (1993) Functional analysis of the γ-glutamylcysteine synthetase of *Escherichia coli* B: effect of substitution of His-150 to Ala. *Appl. Microbiol. Biotechnol.* 38(4):473-477.